



Structural dielectric and magnetic properties of $(1-x)$ BiFeO_3 - $x\text{Ba}_{0.9}\text{Ca}_{0.1}\text{Ti}_{0.9}\text{Sn}_{0.1}\text{O}_3$ ceramics



F. Mizouri ^{a,*}, I. Kallel ^a, N. Abdelmoula ^a, D. Mezzane ^b, H. Khemakhem ^a

^a Laboratory of Multifunctional Materials and Applications (LaMMA), (LR16ES18), Faculty of Sciences of Sfax, University of Sfax, B.P. 1171, 3000, Sfax, Tunisia

^b LMCN, F.S.T.G., University Cadi Ayyad, Marrakech, Morocco

ARTICLE INFO

Article history:

Received 14 June 2017

Received in revised form

3 October 2017

Accepted 9 October 2017

Available online 13 October 2017

Keywords:

Ceramics

Structural properties

Raman spectroscopy

Dielectric properties

Magnetization properties

Hysteresis loop

ABSTRACT

$(1-x)\text{BiFeO}_3$ - $x\text{Ba}_{0.9}\text{Ca}_{0.1}\text{Ti}_{0.9}\text{Sn}_{0.1}\text{O}_3$ ($0.1 < x \leq 0.5$) ceramics are synthesized by conventional solid-state reaction method. These ceramics are characterized by X-ray diffraction, Raman spectroscopy, dielectric and magnetic measurements. X-ray diffraction data refined via Reitveld method revealed that the crystal structure changes from biphasic structures ($R3c + Pnma$) for $x = 0.1$; $x = 0.2$ and $x = 0.3$ with different percentages to orthorhombic ($Pnma$) for $x = 0.4$ and $x = 0.5$, with $(\text{Ba}_{0.9}\text{Ca}_{0.1}\text{Ti}_{0.9}\text{Sn}_{0.1})$ substitution. These results were confirmed by Raman spectroscopy analysis. Moreover, $\text{Ba}_{0.9}\text{Ca}_{0.1}\text{Ti}_{0.9}\text{Sn}_{0.1}\text{O}_3$ doped BiFeO_3 significantly reduces electric leakage and enhances dielectric properties. The obtained hysteresis loop (M-H) indicates that magnetization was enhanced and the maximum value of remnant magnetization occurred at $x = 0.2$ with $M_r = 0.163$ emu/g. This can be explained by the suppression of the cycloid spin structure. A further increase in the substitution percentage beyond the sample $x = 0.20$ caused a large reduction in residual magnetization due to the dominant participation of collinear antiferromagnetic scheduling in the $Pnma$ space group.

© 2017 Elsevier B.V. All rights reserved.

1. Introduction

Possessing the ability to combine two or more of ferroic primary properties in the same phase, multiferroic materials may have a magneto-electric effect, where in the magnetization of the material can be manipulated by applying electric fields and vice versa. Therefore, these materials are already mass produced for various applications in multifunction sensors, actuators, data storage, electrically controlled microwave phase shifters, magnetic field sensors broadband, and magneto-electric memory cells [1,2]. In recent years, since it became one of the most investigated multiferroic materials, bismuth ferrite (BFO) has been raising much interest these days [1–3]. Additionally, bismuth ferrite (BiFeO_3) is considered among the rarest single phase multiferroic materials that simultaneously exhibit ferroelastic, ferroelectric and antiferromagnetic properties at room temperature [4]. Owing to its high phase transition temperature (Curie temperature (T_C) ~ 830 °C and its Neel temperature (T_N) ~ 370 °C) further supports our choice of this bismuth ferrite. It is commonly known that, at room temperature, BiFeO_3 crystallizes in a rhombohedral structure with $R3c$

space group [5]. A G-type antiferromagnetic spin configuration with a canted structure results from the partially filled orbitals of the Fe ions [1,6]. Superexchange interaction between the Fe^{3+} cations with half-filled and localized d^5 ($t_{2g}^3e_g^2$) electronic configuration with five unpaired electrons lead to the magnetic ordering in BiFeO_3 . A G-type canted antiferromagnetic structure of BiFeO_3 was established by Neutron-scattering studies [7]. However, despite the canted G-type antiferromagnetic structure, bulk BiFeO_3 does not display magnetization owing to the superposition of an incommensurate cycloidal modulation of the spins with an approximate wavelength of 620 Å [7]. Observing linear magnetoelectric coupling requires that both remnant polarization and remnant magnetization have the same material. BiFeO_3 can also show a linear magnetoelectric coupling, if the weak ferromagnetism, on account of the spin canting in BiFeO_3 , can be recovered by destroying the spin cycloid [8]. Among the various options for destroying the spin cycloid, solid solution formation with other perovskite oxides proved to be quite effective in releasing the latent weak remnant magnetization of BiFeO_3 in the range of $M_r = 0.1$ – 0.3 emu/g [9,10].

Theoretically speaking, it is expected that BFO, has a large spontaneous polarization (~ 100 $\mu\text{C}/\text{cm}^2$). However, due to its low resistivity at room temperature, bulk BFO synthesized by rapid phase sintering displays only a spontaneous polarization of 8.9 $\mu\text{C}/$

* Corresponding author.

E-mail address: mizourifarhat@yahoo.fr (F. Mizouri).

cm^2 under an applied electric field of 100 kV/cm [11]. It was so difficult to prepare BiFeO_3 in the bulk form without traces of impurities. Indeed, Sosnowska et al. [12] observed an impurity peak of $\text{Bi}_2\text{Fe}_4\text{O}_9$. This was also noted by Tabares-Munoz et al. [13] with the $\text{Bi}_{46}\text{Fe}_2\text{O}_{72}$ material. Therefore, BiFeO_3 - ABO_3 solid-solution systems such as PbTiO_3 [14], BaTiO_3 [15,16] and NaNbO_3 [17] and SrTiO_3 [18], have drawn considerable attention as a means to increase structural stability. Besides, it has been reported that an enhancement in the electrical or magnetic properties was spotted by forming the solid solution of BFO and some ferroelectric materials [19,20]. Substitution into the A and/or B sites of the perovskite structure of parent BiFeO_3 was found to be an effective method to enhance ferroelectricity and improve the magnetic properties and magnetoelectric coupling. However, there has been no discussion regarding the effect of BCTS doped BFO on physical properties. In the present study, $(1-x)\text{BiFeO}_3$ - $x\text{Ba}_{0.9}\text{Ca}_{0.1}\text{Ti}_{0.9}\text{Sn}_{0.1}\text{O}_3$ ceramics [(1-x)BFO-xBCTS] are synthesized by a conventional solid state reaction method over a wide range of compositions ($x = 0.1$ – 0.5) to systematically investigate their structure, and magnetic properties. The structure-property relationships and possible mechanism are also discussed.

2. Experimental

The $(1-x)\text{BiFeO}_3$ - $x\text{Ba}_{0.9}\text{Ca}_{0.1}\text{Ti}_{0.9}\text{Sn}_{0.1}\text{O}_3$ ceramics were prepared by a conventional solid-state reaction method. This system can be noted by $\text{Bi}_{1-x}(\text{Ba}_{0.9}\text{Ca}_{0.1})_x\text{Fe}_{1-x}(\text{Ti}_{0.9}\text{Sn}_{0.1})_x\text{O}_3$ stoichiometric formula. The precursor oxides Bi_2O_3 (99%), Fe_2O_3 (99%), BaCO_3 (99%), CaCO_3 (99.99%), SnO_2 (99%), and TiO_2 (99%) were carefully weighed in stoichiometric ratio and thoroughly wet mixed by ball milling in alcohol for 24 h. The powders were dried and calcined at 600 °C and 700 °C for 4 h. Afterwards, the resultant mixtures were dried and pressed into disks with diameters of 10 mm under 10 MPa. The disks were sintered for 4 h at optimized temperatures 850, 900, 950, 1000 and 1050 °C for $x = 0.1, 0.2, 0.3, 0.4$ and 0.5 , respectively.

Crystal structure was examined via an X-ray diffraction meter with a $\text{CuK}_{\alpha 1}$ radiation ($\lambda = 1.54178\text{\AA}$) (XRD, D8 Advance, Bruker Inc. Raman scattering data were collected in the frequency range of 50–1000 cm^{-1} using a Raman spectrometer (HoribaHR800, Jobin Yvon). The dielectric measurements were studied using LCR meter HP 4284A. The temperature and frequency ranges were between 300 K and 800 K and 100 Hz–100 kHz, respectively. The density of

the leakage current (J) was collected by KEITHLEY 2410. Source Measure Unit, Source Meter, ± 200 mV to ± 1 kV, $1\ \mu\text{A}$ to $\pm 1\text{A}$, 20 W.

Magnetization measurements vs. temperature (T) in an applied magnetic field of 0.05 T and magnetization (M) vs. magnetic field were measured by means of a BS2 magnetometer.

3. Results and discussions

3.1. Phase purity

XRD patterns for all the samples $(1-x)\text{BiFeO}_3$ - $x\text{Ba}_{0.9}\text{Ca}_{0.1}\text{Ti}_{0.9}\text{Sn}_{0.1}\text{O}_3$ with $x = 0.1; 0.2; 0.3; 0.4$ and 0.5 are shown in Fig. 1. A small amount of impurity phases of $\text{Bi}_2\text{Fe}_4\text{O}_9$ and $\text{Bi}_{25}\text{FeO}_{40}$ was spotted from the XRD pattern for $x = 0.1$ and $x = 0.2$ [21,22]. The impurities were deleted as $\text{Ba}_{0.9}\text{Ca}_{0.1}\text{Ti}_{0.9}\text{Sn}_{0.1}\text{O}_3$ increased. Rietveld refinement of X-ray diffraction confirms the co-presence of rhombohedral $R3c$ and orthorhombic $Pnma$ phases for $x = 0.1$ (96.93% $R3c$ + 3.07% $Pnma$); $x = 0.2$ (95.54% $R3c$ + 4.46% $Pnma$) and 0.3 (17% $R3c$ + 83% $Pnma$) with reasonable refinement agreement factors ($\chi^2 = 1.51; 1.58$ and 1.59 respectively). The predominant rhombohedral structure for $x = 0.1$ and $x = 0.2$ is characterized by the doublet of the highest intensity peaks reflections (104) and (110) at $2\theta = 31.8^\circ$ and 32.1° , as indicated in Fig. 1b. The disappearance of the peak (113) at $2\theta = 37.8^\circ$ characteristic of $R3c$ phase was detected with the increase in substitution to $x = 0.3$ (Fig. 1a), caused by the coexistence of orthorhombic ($Pnma$) with dominating fraction close to 83% and rhombohedral ($R3c$) symmetry. When increasing the $\text{Ba}_{0.9}\text{Ca}_{0.1}\text{Ti}_{0.9}\text{Sn}_{0.1}\text{O}_3$ content, all the doublets overlap to supply a single peak, which is clearly visible in XRD patterns of $(1-x)\text{BFO}$ - $x\text{Ba}_{0.9}\text{Ca}_{0.1}\text{Ti}_{0.9}\text{Sn}_{0.1}\text{O}_3$ for $x = 0.4$ and $x = 0.5$. Moreover, the typical reflections of $Pnma$ space group as (111) at $2\theta = 25.5^\circ$ and three new superlattice reflections, such as (102), (131) and (212) at $2\theta = 35.6^\circ, 41.9^\circ$, and 47.9° characteristic of the anti-parallel cation displacements of $Pnma$ space group appeared in $x = 0.4$ – 0.5 (Fig. 1a). This shows that the compositions with $x = 0.4$ and $x = 0.5$ acquire an orthorhombic $Pnma$ symmetry. The above observations clearly display the structural transition from the predominant rhombohedral ($x = 0.1$ and $x = 0.2$) to orthorhombic phase for $x = 0.4$ and $x = 0.5$. More precisely, the contribution of $Pnma$ phase is $\sim 83\%$ for $x = 0.3$, until passing completely to the $Pnma$ phase for $x = 0.4$. Then, $x = 0.3$ can be defined as an intermediate composition. A similar behavior was detected in Bi_{1-x}

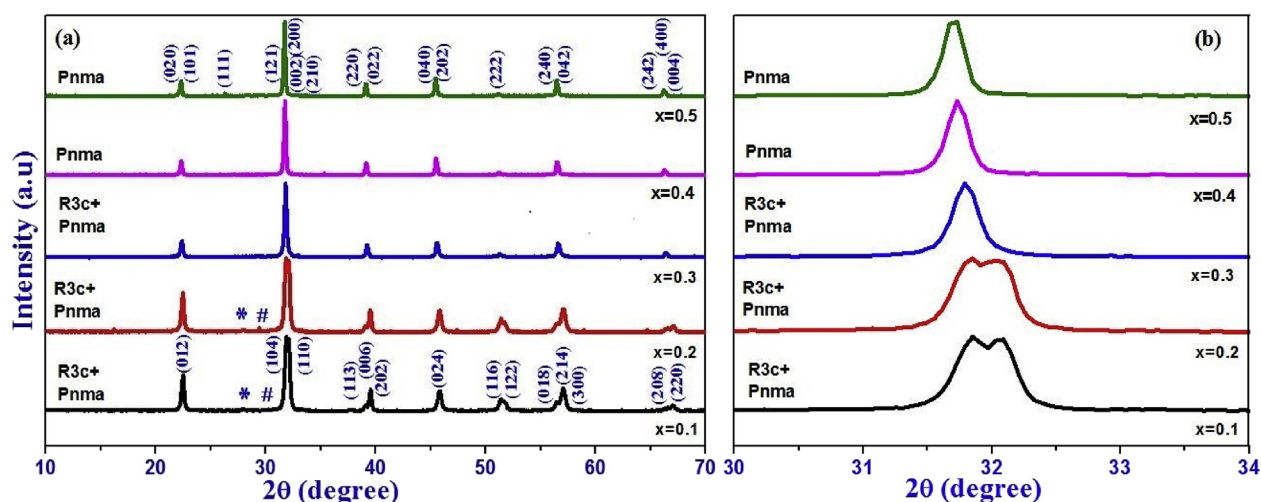


Fig. 1. (a) X-ray diffraction pattern for $(1-x)\text{BiFeO}_3$ - $x\text{Ba}_{0.9}\text{Ca}_{0.1}\text{Ti}_{0.9}\text{Sn}_{0.1}\text{O}_3$ ceramics (a) with $x = 0.1, 0.2, 0.3, 0.4$ and 0.5 , (b) the magnification in the 2θ range from (32°) .

Download English Version:

<https://daneshyari.com/en/article/5458061>

Download Persian Version:

<https://daneshyari.com/article/5458061>

[Daneshyari.com](https://daneshyari.com)